Sensorless control of PM-assisted SyR motors

Candidate: Salvatore Domenico MISTRETTA   **Supervisor:** Prof. Gianmario PELLEGRINO
Advisor: Anantaram VARATHARAJAN

Abstract—The aim of the work is the simulation and experimental validation of the sensorless control of a permanent magnet (PM)-assisted Synchronous Reluctance (SyR) motor drive, for general purpose variable speed applications. The sensorless control method is based on two stages: I-f control and sensorless field oriented control (FOC). The former is an open-loop speed control, used only to start and stop the drive, where stator currents are imposed in an arbitrary reference frame having a frequency ramp variation. The FOC is activated when motor speed is higher than a fixed threshold. During this stage, the speed and position feedback is estimated by a flux and position observer based on the flux Cross Product sensorless method. Some precautions are adopted when transitioning between the two speed regions, in order to ensure a smooth speed transient. The developed sensorless techniques are fully validated with simulation and experimental results on a 7.5 hp IE4 motor by ABB, showing good performance and robustness both at no load and under rated load.

I. INTRODUCTION

During the last 50 years, the global electricity consumption has grown by four times. Following this trend, the global policy makers are encouraging the replacement of direct online low efficiency motors with variable speed drives of higher efficiency: permanent magnet synchronous machines (PMSMs) are a valid way to achieve this aim. In particular, PM-assisted SyR motors are much cheaper than other PMSMs, due to low amount of PM allocated in rotor. In order to reduce the drive cost, the speed/position transducer is eliminated, improving also reliability. Many solutions were proposed in the literature for the sensorless control of PMSMs; they can be divided in two main categories: fundamental model sensorless techniques, based on back-EMF and its integration, and saliency based sensorless techniques, using high frequency excitation.

II. ADOPTED SENSORLESS CONTROL STRATEGY

The strategy adopted to sensorless control a PM-assisted SyR motor is organized as a state machine, with only two operating states: I-f control and sensorless FOC. At the start-up, the drive is controlled by I-f control. If reference speed ω^* overcomes speed threshold ω_{up}, the state machine abruptly jumps to sensorless FOC, adopting some precautions during up transition. A similar procedure is used for decelerating back to stop the motor. In fact, if the estimated speed $\hat{\omega}$ is lower than speed threshold ω_{down}, the control jumps back to I-f strategy, adopting additional precautions during downwards transition. In particular, the two speed threshold are such that $\omega_{up} > \omega_{down}$. Figure 1

illustrates philosophy of the proposed sensorless control method.
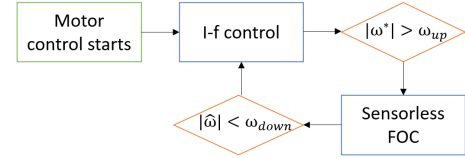

Figure 1: Block diagram for sensorless control with open-loop starting

A. I-f control and sensorless FOC overview

In I-f control, motor speed is related to the imposed frequency of the reference current vector. Being an open-loop speed control, it does not need any speed information, though the dynamics is modest. However this control is only used to start and stop the drive. On the other hand, sensorless FOC is a closed loop speed control where speed and position angle feedbacks are properly estimated. During this operating state, reference speed is compared to the estimated one: error becomes input of PI speed controller, giving as output the torque needed to regulate the speed. This signal is processed by a linear interpolation of the maximum torque per amper (MTPA) look-up table (LUT), providing as output the desired d-q reference current. Therefore, the drive spends the minimum motor current for a given torque, increasing efficiency. Figure 2 presents the complete block diagram: position 1 (red) refers to I-f control while position 2 (green) refers to sensorless FOC.
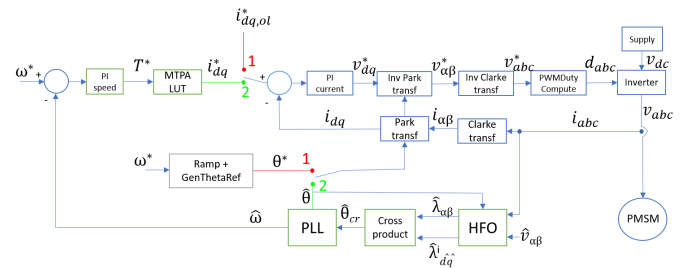

Figure 2: Control scheme of the adopted sensorless strategy

B. Speed and position estimation

In order to properly estimate the speed/position information, knowledge of the flux linkage is needed. It can be estimated thanks to a hybrid flux observer (Figure 3), based on back-EMF integral with a compensating signal which is the difference between voltage model and current model (flux maps output).

The flux cross product position observer is the heart of the implemented strategy. It retrieves the electrical rotor position information starting from estimated flux in $\alpha\beta$ and the current-model flux in dq as:

$$\begin{cases} \sin(\hat{\theta}_{cr}) = \dfrac{\hat{\lambda}_{\hat{d}}^i \hat{\lambda}_\beta - \hat{\lambda}_\alpha \hat{\lambda}_{\hat{q}}^i}{\lambda^2} \\[3mm] \cos(\hat{\theta}_{cr}) = \dfrac{\hat{\lambda}_{\hat{d}}^i \hat{\lambda}_\alpha + \hat{\lambda}_\beta \hat{\lambda}_{\hat{q}}^i}{\lambda^2} \end{cases} \quad (1)$$

The last step consists in speed estimation $\hat{\omega}$: PLL is used to achieve this aim. At low speeds ($\omega^* < \omega_{act}$), PLL is partially active: position error signal ϵ is fixed to zero, while the integral part of the PI controller is set to ω^*. Therefore, speed and position estimations are respectively equal to the reference ones.
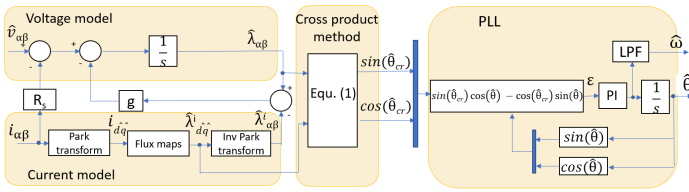

Figure 3: Speed and position estimation block diagram

C. Transition strategy

To avoid speed discontinuity during transition, some precautions are adopted. As far as upwards transition is concerned, when the jump occurs the integral part of PI speed controller is initialized to estimated torque:

$$\hat{T} = \frac{3}{2}p(\hat{\lambda}_\alpha i_\beta - \hat{\lambda}_\beta i_\alpha) \quad (2)$$

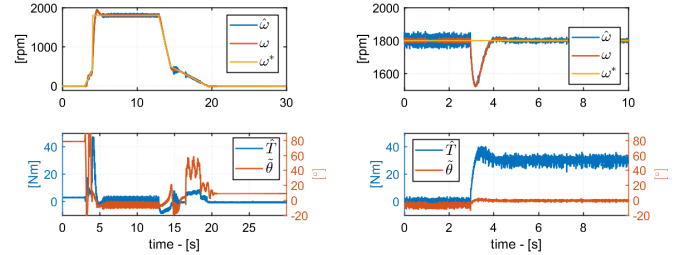For downwards transition, restrictions are more severe:
- Reference current vector located in zero torque locus during I-f control, to avoid torque discontinuity;
- Reference angle θ^* initialized to the estimated angle $\hat{\theta}$, just before the jump;
- Limited slew-rate deceleration near transition speed ω_{down}.

III. Experimental results

The experimental test platform (Fig. 5) consists of the 7.5 hp ABB motor, driven by three-phase two-levels voltage source inverter ($v_{dc} = 360V$), a load drive to impose load torque and the dSPACE 1005 platform. Regarding calibration, the PI current controllers parameters are set to: $k_p = 20$ $k_i = 2000$; speed bandwidth is fixed to 2.5 Hz while PLL poles position to 15 Hz; the crossover angular frequency g is imposed to $2\pi10$ rad/s; threshold speeds: $\omega_{up} = 400$ rpm, $\omega_{down} = 300$ rpm, $\omega_{act} = 100$ rpm; estimate speed is low pass filtered at 25 Hz cut-off frequency. Reference current vector components are located in zero torque locus: $i_{d,ol}^* = 10A$ and $i_{q,ol}^* = -7A$. The limits of the speed reference slew-rate for the motor under test are identified experimentally as:

- 100 rpm/s during acceleration/deceleration in I-f control;
- 15000 rpm/s during acceleration in sensorless FOC;
- 800 rpm/s during deceleration in sensorless FOC, until the speed 500 rpm and reduced to 100 rpm/s henceforth.

The performance of the adopted sensorless control system is experimentally investigated in different cases, among which acceleration/deceleration at no load and imposition of rated torque load at 1800 rpm are shown in Figs. 4a and 4b, respectively.

(a) *Acceleration and deceleration test at no load*

(b) *Imposition of rated torque (29.8Nm) at rated speed*

Figure 4: Experimental results from top to bottom: estimated speed $\hat{\omega}$, motor speed ω, reference speed ω^*, estimated torque $\hat{T}$, position error $\hat{\theta}$

In both tests, the speed dynamic response is satisfactory. In FOC, the position error $\hat{\theta}$ is less than 5° under load. Higher load torque improves the position estimation accuracy, due to higher flux linkage and a better signal to noise ratio. Moreover, left figure demonstrates the successful transitions, where a smooth speed characteristic is obtained. The control is further validated with other tests such as: overload test (145% of rated torque) and starting test under reduced load (until 40% of rated torque).

IV. Conclusion

In this thesis, the sensorless control of an industrial PM-SyR machine was designed and implemented. Though the transitions between the I-f and FOC speed regions are abrupt, convergence is always ensured thanks to the precautions adopted. The core of the FOC lives in the combination of the hybrid flux observer, Cross Product method and the PLL: thanks to a proper calibration, position error did not exceed ±10° in the comprehensive test campaign, including overload conditions. The calibration rules are valid in general and easy to replicate on PM-SyR machines of different size.
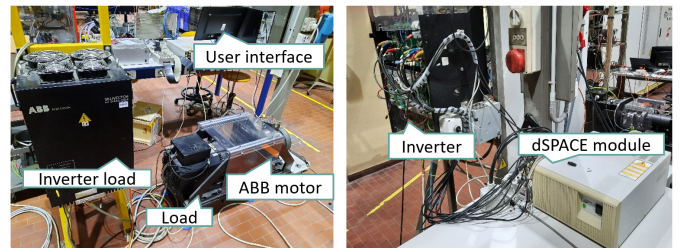

Figure 5: Experimental test platform